

# MMRINET: EFFICIENT MAMBA-BASED SEGMENTATION WITH DUAL-PATH REFINEMENT FOR LOW-RESOURCE MRI ANALYSIS

*Abdelrahman Elsayed\**, *Ahmed Jaheen\**, and *Mohammad Yaqub*

Mohamed bin Zayed University of Artificial Intelligence (MBZUAI)  
Abu Dhabi, United Arab Emirates

{[abdelrahman.elsayed](mailto:abdelrahman.elsayed@mbzuai.ac.ae), [ahmed.jaheen](mailto:ahmed.jaheen@mbzuai.ac.ae), [mohammad.yaqub](mailto:mohammad.yaqub@mbzuai.ac.ae)}@mbzuai.ac.ae  
<https://mbzuai.ac.ae>

## ABSTRACT

Automated brain tumor segmentation in multi-parametric MRI remains challenging in resource-constrained settings where deep 3D networks are computationally prohibitive. We propose MMRINET, a lightweight architecture that replaces quadratic-complexity attention with linear-complexity Mamba state-space models for efficient volumetric context modeling. Novel Dual-Path Feature Refinement (DPFR) modules maximize feature diversity without additional data requirements, while Progressive Feature Aggregation (PFA) enables effective multi-scale fusion. In the BraTS-Lighthouse SSA 2025, our model achieves strong performance with an average Dice score of **(0.752)** and an average HD95 of **(12.23)** with only  $\sim 2.5$ M parameters, demonstrating efficient and accurate segmentation suitable for low-resource clinical environments. Our GitHub repository can be accessed here: [github.com/BioMedIA-MBZUAI/MMRINET](https://github.com/BioMedIA-MBZUAI/MMRINET).

**Index Terms**— Brain MRI, Tumor segmentation, Mamba, U-Net, State-space models, and Computational efficiency

## 1. INTRODUCTION

Glioma segmentation from multi-parametric MRI is critical for diagnosis and treatment planning, yet manual delineation is time-consuming and prone to inter-observer variability. Deep learning architectures, particularly U-Net and its 3D extensions [1, 2, 3], have become standard in medical image segmentation. However, these volumetric networks rely on deep encoders and extensive GPU resources, which hinder deployment in resource-constrained clinical settings such as those across sub-Saharan Africa (SSA), the focus region of the BraTS-Lighthouse SSA challenge. To enhance segmentation performance, subsequent Transformer-based architectures such as UNETR [4] and SwinUNETR [5] introduced self-attention mechanisms to capture long-range dependencies and global context, achieving good results on benchmark datasets like BraTS [6], though performance degrades in SSA settings due to limited training data and scanner variability. Yet, these models incur quadratic computational cost with respect to input size and depend on large-scale, high-quality datasets that are often unavailable in developing regions.

To improve model robustness and accessibility, several studies have explored lightweight architectural and training optimizations for brain tumor segmentation. CNN variants such as Attention U-Net [7], UNet++ [8], and Efficient-UNet [9] introduced hierarchical skip connections, compound scaling, and parameter pruning to

enhance efficiency without compromising accuracy. Parallel efforts have explored domain adaptation and self-supervised learning techniques [10, 11, 12] to improve generalization under data scarcity and scanner variability. However, despite these improvements, most models remain reliant on extensive pretraining or heavy encoder backbones, limiting their real-world applicability in hospitals with low-field MRI scanners and restricted computation.

Recent state-space models offer promising alternatives. Mamba [13] achieves linear complexity relative to sequence length, enabling efficient long-range dependency modeling. Medical imaging adaptations like U-Mamba [14] and SegMamba [15] have demonstrated competitive performance on 3D volumetric segmentation by integrating SSM blocks within U-Net-like architectures. Group-wise state-space modeling [16] has further enhanced parameter efficiency through channel partitioning and multi-directional scanning. However, architectural innovations that combine these efficiency gains with explicit designs for feature diversity and multi-scale fusion under extreme data constraints remain underexplored.

Efforts dedicated to SSA brain MRI analysis [6, 17] revealed substantial performance degradation when models pretrained on Western datasets are applied to African cohorts, primarily due to scanner variability, noise, and limited annotated data. Initiatives such as BraTS-Africa 2023 and BraTS-Lighthouse SSA 2025 highlight the urgent need for architectures that remain both accurate and efficient under constrained data and hardware conditions. However, recent competitive methods in the BraTS SSA challenge [18, 19, 20] remain parameter-heavy and computationally expensive, lacking mechanisms for efficient context modeling and domain robustness, limitations that our proposed **MMRINET** directly addresses. Motivated by the efficiency of Mamba-based architectures and the specific constraints of SSA clinical settings, we introduce **MMRINET**, explicitly designed for low-resource scenarios through three key innovations: (i) a **Modulated GroupMamba-based bottleneck [16]** that applies multi-directional scanning across depth, height, and width axes to preserve 3D spatial coherence while achieving linear-complexity global modeling, (ii) **Dual-Path Feature Refinement (DPFR)** that extracts complementary detail and context features to maximize diversity under limited data, and (iii) **Progressive Feature Aggregation (PFA)** for effective multi-scale fusion. With only  $\sim 2.5$ M parameters and deep supervision, our model achieves competitive BraTS-Lighthouse SSA 2025 performance (0.75 Dice, 12.23 mm HD95) while maintaining efficiency suitable for resource-limited clinical deployment.

\*Equal contribution; names are presented alphabetically

## 2. METHODS

### 2.1. Datasets

Our experiments are conducted mainly on the dataset released in the BraTS–Lighthouse 2025 Challenge for the Sub-Saharan African Population [6] [17]. This is the **only public** dataset consists of 3D multi-parametric MRI scans collected in sub-Saharan Africa, primarily from clinical sites in Nigeria. Each case includes the four standard MRI modalities: T1, T1ce, T2, and FLAIR with expert-annotated tumor masks. The cohort comprises 60 training and 35 validation cases. It reflects real-world variability caused by low-field MRI scanners, diverse patient demographics, and higher levels of noise, making it particularly challenging and clinically relevant.

### 2.2. Data Preprocessing and Augmentation

All MRI volumes undergo standardized preprocessing: intensities are normalized per modality using non-zero voxels with channel-wise statistics. Random spatial crops of size  $160 \times 160 \times 128$  are extracted during training to fit GPU memory constraints and encourage the model to learn from diverse volumetric contexts.

To improve model robustness and generalization, we apply extensive data augmentation during training. Our augmentation pipeline includes: (i) random spatial flipping along all three axes with probability 0.5, (ii) random intensity scaling by a factor of  $\pm 10\%$ , and (iii) random intensity shifts by  $\pm 10\%$ . These transformations preserve anatomical structure while introducing realistic intensity variations that mimic scanner variability and acquisition artifacts.

### 2.3. Network Architecture

MMRINet follows a U-Net encoder-decoder structure optimized for low-resource 3D medical image segmentation. Key innovations include: (i) Mamba-based bottleneck for efficient global modeling, (ii) Dual-Path Feature Refinement (DPFR) in decoders, and (iii) Progressive Feature Aggregation (PFA). The architecture overview is shown in Figure 1.

#### 2.3.1. Encoder

The encoder comprises four stages with *BasicBlock3D* residual units and strided downsampling. Starting from  $C_{in} = 4$  input channels, features expand to 16, 32, 64, and 128 channels while spatial resolution reduces to  $D/2$ ,  $D/4$ ,  $D/8$ , and maintains  $D/8$  respectively. Each stage generates skip connections for decoder fusion. All blocks use batch normalization, ReLU, and dropout (0.05).

#### 2.3.2. Mamba Bottleneck

At  $D/8 \times H/8 \times W/8$  resolution (128ch), the bottleneck employs: (1) **GroupMamba3D** extended from [16] with  $G = 4$  groups and  $d_{ssm} = 32$ . Unlike standard Mamba, GroupMamba partitions channels into groups and applies directional scanning along  $H$ ,  $W$ ,  $D$ , and  $HW$  axes independently, enabling parallel capture of anisotropic volumetric dependencies. Each group undergoes depthwise convolution, state-space projection, and layer normalization, followed by cross-group modulation. This reduces parameters by  $1/G$  while maintaining global receptive fields, crucial for efficient  $128^3$  volume processing. (2) **Channel Attention** (squeeze-excitation,  $r = 8$ ) for feature recalibration, and (3) **BasicBlock3D** for refinement as shown in Figure 2.

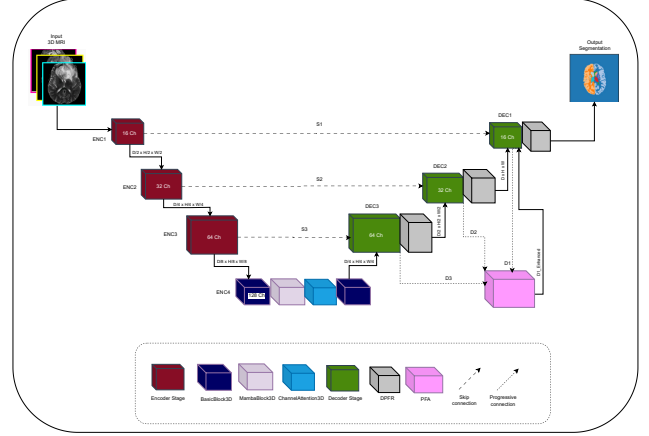


**Fig. 1.** Overview of MMRINet Architecture. It combines a convolutional encoder with a Mamba-based bottleneck for efficient global context, and a decoder with Dual-Path Feature Refinement (DPFR) and Progressive Feature Aggregation (PFA) for multi-scale segmentation.

#### 2.3.3. Decoder with DPFR

Three decoder stages progressively upsample via transposed convolution, concatenate encoder skips, and fuse through *BasicBlock3D*. Each stage includes our novel **Dual-Path Feature Refinement (DPFR)** as shown in Figure 2:

- **Detail Path:** Standard  $3 \times 3 \times 3$  depthwise-separable conv preserves fine features.
- **Context Path:** Dilated conv (dilation=2) captures broader patterns.
- **Cross-Interaction:** Concatenated paths exchange information via  $1 \times 1 \times 1$  conv.
- **Adaptive Gating:** Learns to weight detail vs. context through global pooling and softmax.

DPFR maximizes feature diversity without additional data, acting as implicit ensemble with self-supervised regularization.

#### 2.3.4. Progressive Feature Aggregation and Output

**PFA** hierarchically fuses multi-scale decoder features where  $\mathcal{F}_{agg} = \mathcal{U}(\mathcal{U}(\mathcal{D}_3) + \mathcal{D}_2) + \mathcal{D}_1$ , where  $\mathcal{U}$  denotes learned upsampling. Final output combines  $\mathcal{F}_{agg}$  with  $\mathcal{D}_1$  via residual connection, followed by *BasicBlock3D* refinement and  $1 \times 1 \times 1$  conv to  $C_{out} = 3$  classes. **Deep Supervision:** During training, auxiliary heads at  $\mathcal{D}_3, \mathcal{D}_2, \mathcal{D}_1$  provide multi-level supervision with weighted loss.

### 2.4. Loss Function

We employ a combined Dice-Focal loss to address the class imbalance inherent in brain tumor segmentation, where lesion regions constitute a small fraction of the total brain volume. The Dice-Focal loss is formulated as:

$$\mathcal{L}_{seg} = \mathcal{L}_{Dice} + \mathcal{L}_{Focal} \quad (1)$$

where the Dice loss measures the overlap between predicted and ground-truth masks, and the Focal loss down-weights well-classified examples while emphasizing hard, misclassified regions. We set the focal parameter  $\gamma = 2.0$  to strongly focus on challenging samples.

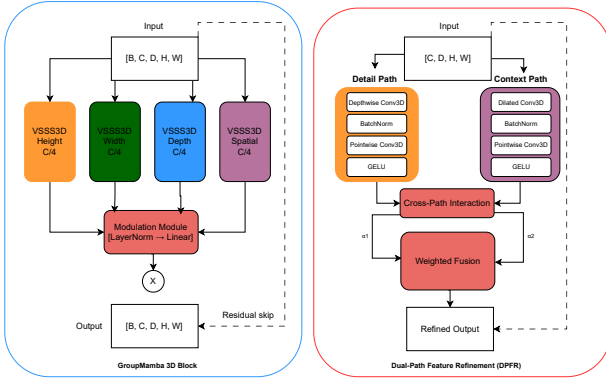


**Fig. 2. Key architectural components of MMRINet.** (Left) The **GroupMamba 3D Block** models long-range spatial dependencies efficiently via group-wise state-space mixing and a lightweight modulation layer. (Right) The **Dual-Path Feature Refinement (DPFR)** module enhances decoder representations by combining fine-grained detail and coarse contextual features through adaptive gating and weighted fusion.

The loss is computed with sigmoid activation and averaged across the batch to stabilize training dynamics.

To leverage intermediate representations and improve gradient flow through the deep network, we apply deep supervision at multiple decoder stages. Specifically, MMRINet produces four outputs: three auxiliary predictions ( $out_1$ ,  $out_2$ ,  $out_3$ ) from intermediate decoder levels and one final prediction. The total training loss is a weighted sum:

$$\mathcal{L} = 0.2\mathcal{L}(out_1) + 0.3\mathcal{L}(out_2) + 0.3\mathcal{L}(out_3) + 0.2\mathcal{L}(final) \quad (2)$$

which encourages the network to learn meaningful representations at multiple levels of abstraction. During inference, only the final prediction is used, ensuring efficient and accurate segmentation while benefiting from the deep supervision during training.

### 3. EXPERIMENTAL SETUP

#### 3.1. Training Configuration

To maintain consistency with our low-resource design, MMRINet was trained on a single NVIDIA RTX A6000 GPU using mixed-precision (FP16) to reduce memory and computation cost. The model converged within 100 epochs using the AdamW optimizer with an initial learning rate of  $3 \times 10^{-4}$  and weight decay of  $1 \times 10^{-2}$ . A lightweight schedule-free learning rate strategy [21] was applied ( $r=1.0$ ,  $weight\_lr\_power=0.5$ ) to promote stable convergence without additional epochs.

We employed a small batch size of 2 volumes due to GPU memory constraints. Training incorporated deep supervision (Section 2.4) to enhance gradient flow in this compact architecture.

#### 3.2. Evaluation Metrics

Performance is evaluated using Dice Similarity Coefficient (DSC) and 95th percentile Hausdorff Distance (HD95) for three tumor sub-regions: **Enhancing Tumor (ET)**, **Tumor Core (TC)**, and **Whole Tumor (WT)**. Overall performance is reported as mean DSC across all regions.

#### 3.3. Baselines

We evaluated the BraTS-Lighthouse SSA 2025 dataset and implemented all baseline models using MONAI [22] with parameters optimized for small datasets to avoid overfitting. For SegMamba, we used the original implementation with similar parameter tuning to ensure fair comparison. All models are trained under identical hardware constraints and data augmentation pipelines.

## 4. RESULTS

#### 4.1. Quantitative Evaluation

Table 1 summarizes the segmentation performance of MMRINet on the BraTS-Lighthouse SSA 2025 validation set. Our model achieves an average Dice score of **75.2%** and good-performing HD95 with an average of **12.23** across the three tumor regions.

**Table 1.** Segmentation performance on the validation set.

Model	DSC (%)				HD95 (mm)			
	ET	TC	WT	AVG	ET	TC	WT	AVG
UNETR [4]	0.64	0.62	0.77	0.68	56.83	18.14	30.33	35.10
Swin UNETR [23]	0.62	0.62	0.81	0.68	33.43	40.72	60.38	44.84
SegMamba [15]	0.62	0.64	0.82	0.69	22.79	12.55	15.11	20.15
SegResNet3D [24]	0.63	0.66	0.82	0.70	62.45	12.92	16.21	30.53
MONAI 3D U-Net [1]	0.68	0.71	0.80	0.73	<b>9.57</b>	22.13	21.95	17.88
<b>MMRINet (Ours)</b>	<b>0.69</b>	<b>0.73</b>	<b>0.84</b>	<b>0.75</b>	16.21	<b>8.12</b>	<b>12.36</b>	<b>12.23</b>

#### 4.2. Computational Efficiency

A key advantage of MMRINet is its computational efficiency compared to standard 3D U-Net baselines. Table 2 presents a comparison of model size and initial feature dimension or channels.

**Table 2.** Computational efficiency comparison with trainable parameters (M)

Model	Params (M)
SegMamba	18.8
UNETR	13.2
SegResNet3D	4.7
Swin UNETR	4.1
3D U-Net	2.0
<b>MMRINet (Ours)</b>	<b>2.5</b>

MMRINet achieves remarkable computational efficiency compared to transformer-based and hybrid 3D segmentation architectures. As summarized in Table 2, MMRINet contains only 2.5 million parameters, 80% fewer than UNETR and SegMamba, nearly 40% fewer than Swin UNETR and SegResNet3D. This reduction is achieved without sacrificing segmentation performance, owing to the linear-time Mamba blocks that replace self-attention and the dual-path refinement design that enhances multi-scale contextual learning with minimal overhead.

#### 4.3. Ablation Studies

##### 4.3.1. MMRINet Components

To validate each proposed component, we conduct systematic ablation experiments using the same experimental setup as in our main

results. Table 3 presents component-wise performance. The baseline model (encoder-decoder with Mamba bottleneck, no enhancements) achieves 0.69 Dice and 17.69 mm HD95. Our novel **DPFR module** provides the largest gain (+0.05 Dice, -2.82 mm HD95), validating its dual-path design to maximize feature diversity without additional data. Deep supervision improves gradient flow (+0.02 Dice). Combining DPFR with deep supervision yields 0.75 Dice. The full model achieves best overall performance (0.75 Dice, 12.23 mm HD95), with superior boundary precision indicating **synergistic component interactions**: PFA’s multi-scale aggregation benefits from DPFR’s refined features, while deep supervision stabilizes training across all scales. DPFR adds 0.45M parameters (18% in-

**Table 3.** Component-wise Performance on Validation Set

Configuration	Dice	HD95 (mm)
Baseline (GroupMamba + U-Net)	0.69	18.80
+ Deep Supervision	0.71	17.69
+ DPFR	0.74	17.29
+ DPFR + Deep Sup	0.75	14.87
<b>Full MMRINet</b>	<b>0.75</b>	<b>12.23</b>

crease), deep supervision adds 0.08M (training only), and PFA adds 0.12M. The full 2.5M-parameter model achieves 6% Dice improvement and 35% HD95 improvement over baseline, demonstrating exceptional parameter efficiency compared to UNETR (13.2M) and SegMamba (18.8M). Figure 3 shows MMRINet’s superior boundary delineation and small region sensitivity, particularly for challenging cases with noise and irregular morphology of the SSA dataset.

#### 4.3.2. Qualitative Results

Figure 3 shows representative segmentation examples from the validation set. MMRINet successfully delineates complex tumor morphologies, including irregular boundaries and small enhancing regions, demonstrating robust performance across diverse cases. Figure 3 shows representative segmentation results. Colors: green (WT), blue (ET). The baseline model over-segments ET (larger blue regions) compared to ground truth, while the full MMRINet achieves better specificity and boundary precision in both samples. These improvements demonstrate DPFR’s effectiveness in reducing false positives while maintaining accurate tumor extent delineation.

## 5. DISCUSSION

MMRINet achieves competitive performance with only 2.5M parameters, demonstrating that linear-complexity Mamba blocks effectively replace quadratic-scaling attention mechanisms for 3D medical image segmentation. Our model outperforms all baselines in average Dice (0.75) and HD95 (12.23 mm), with particularly strong improvements in boundary precision (TC and WT HD95) compared to transformer-based approaches. The strong WT performance (0.84) reflects robust whole tumor detection, while the moderate ET score (0.69) highlights the inherent difficulty of delineating small, heterogeneous enhancing regions. Notably, MMRINet achieves these results with more than 80% fewer parameters than bigger models such UNETR and SegMamba, validating our architectural innovations: DPFR maximizes feature diversity without additional data, PFA enables effective multi-scale fusion, and deep supervision stabilizes training in compact architectures. The 2% Dice improvement over MONAI 3D U-Net (2.0M parameters) and

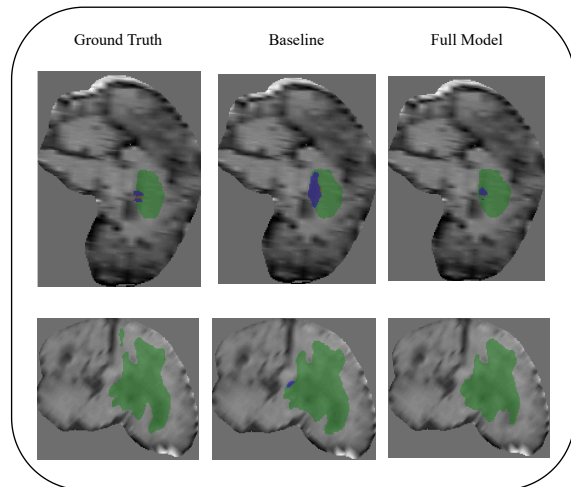


**Fig. 3.** Qualitative segmentation results on BraTS-Lighthouse SSA 2025 validation cases with overlay. Colors: green (WT), blue (ET).

31% HD95 improvement demonstrate that state-space models offer a promising path for resource-constrained clinical deployment, particularly in sub-Saharan Africa where computational efficiency is critical.

## 6. CONCLUSION

We introduced MMRINet, a lightweight Mamba-based architecture for brain tumor segmentation tailored for resource-limited clinical environments. By integrating linear-complexity state-space modeling with Dual-Path Feature Refinement (DPFR) and Progressive Feature Aggregation (PFA), MMRINet balances contextual awareness and fine structural detail, achieving competitive performance (0.75 Dice, 12.23 mm HD95) with only 2.5M parameters. The model surpasses heavier transformer-based baselines while enabling faster convergence and reduced GPU memory usage, validating its suitability for deployment in low-resource hospitals. Future work will expand MMRINet into a multi-task framework integrating tumor grading and survival prediction, with cross-dataset evaluation across BraTS, BraTS-Africa, and clinical data to further assess generalization across scanner conditions. Moreover, we will extend MMRINet to other imaging modalities, leveraging the efficiency of Mamba’s linear-complexity modeling to achieve robust and scalable multi-modal brain tumor analysis across diverse clinical datasets.

## 7. COMPLIANCE WITH ETHICAL STANDARDS

This research study was conducted using publicly available data from the BraTS-Lighthouse SSA 2025 Challenge. The data were fully anonymized and did not contain identifiable human information. No additional ethical approval was required for this study.

## 8. REFERENCES

- [1] Özgün Çiçek, Ahmed Abdulkadir, Soeren S. Lienkamp, Thomas Brox, and Olaf Ronneberger, “3d u-net: Learning

- dense volumetric segmentation from sparse annotation,” in *Medical Image Computing and Computer-Assisted Intervention – MICCAI 2016*, Cham, 2016, pp. 424–432, Springer International Publishing.
- [2] Fausto Milletari, Nassir Navab, and Seyed-Ahmad Ahmadi, “V-net: Fully convolutional neural networks for volumetric medical image segmentation,” in *2016 Fourth International Conference on 3D Vision (3DV)*, 2016, pp. 565–571.
  - [3] Fabian Isensee, Paul F. Jaeger, Simon A. A. Kohl, Jens Petersen, and Klaus H. Maier-Hein, “nnu-net: a self-configuring method for deep learning-based biomedical image segmentation,” *Nature Methods*, vol. 18, no. 2, pp. 203–211, Feb 2021.
  - [4] Ali Hatamizadeh, Yucheng Tang, Vishwesh Nath, Dong Yang, Andriy Myronenko, Bennett Landman, Holger R. Roth, and Daguang Xu, “Unetr: Transformers for 3d medical image segmentation,” in *2022 IEEE/CVF Winter Conference on Applications of Computer Vision (WACV)*, 2022, pp. 1748–1758.
  - [5] Ali Hatamizadeh, Vishwesh Nath, Yun Tang, Dong Yang, Holger Roth, and Daguang Xu, “Swin unetr: Swin transformers for semantic segmentation of brain tumors in mri images,” *BrainLes Workshop, MICCAI*, 2022.
  - [6] Maruf Adewole, Jeffrey D Rudie, Anu Gbadamosi, and et al., “The brats-africa dataset: Expanding the brain tumor segmentation (brats) data to capture african populations,” *Radiology: Artificial Intelligence*, 2025, Accepted April 16.
  - [7] Ozan Oktay, Jo Schlemper, Loic Le Folgoc, Matthew Lee, Mattias Heinrich, Kazunari Misawa, Kensaku Mori, Steven McDonagh, Nils Y Hammerla, Bernhard Kainz, et al., “Attention u-net: Learning where to look for the pancreas,” *arXiv preprint arXiv:1804.03999*, 2018.
  - [8] Zongwei Zhou, Md Mahfuzur Rahman Siddiquee, Nima Tajbakhsh, and Jianming Liang, “Unet++: A nested u-net architecture for medical image segmentation,” in *International workshop on deep learning in medical image analysis*. Springer, 2018, pp. 3–11.
  - [9] Hüseyin Üzen, Muammer Turkoglu, Muzaffer Aslan, and Davut Hanbay, “Depth-wise squeeze and excitation block-based efficient-unet model for surface defect detection,” *The Visual Computer*, vol. 39, no. 5, pp. 1745–1764, 2023.
  - [10] Christian S Perone, Pedro Ballester, Rodrigo C Barros, and Julien Cohen-Adad, “Unsupervised domain adaptation for medical imaging segmentation with self-ensembling,” *NeuroImage*, vol. 194, pp. 1–11, 2019.
  - [11] Ziwei Niu, Shuyi Ouyang, Shiao Xie, Yen-wei Chen, and Lanfen Lin, “A survey on domain generalization for medical image analysis,” *arXiv preprint arXiv:2402.05035*, 2024.
  - [12] Jee Seok Yoon, Kwansook Oh, Yooseung Shin, Maciej A Mazurowski, and Heung-Il Suk, “Domain generalization for medical image analysis: A review,” *Proceedings of the IEEE*, 2024.
  - [13] Albert Gu and Tri Dao, “Mamba: Linear-time sequence modeling with selective state spaces,” 2024.
  - [14] Jun Ma, Feifei Li, and Bo Wang, “U-mamba: Enhancing long-range dependency for biomedical image segmentation,” 2024.
  - [15] Zhaohu Xing, Tian Ye, Yijun Yang, Guang Liu, and Lei Zhu, “Segmamba: Long-range sequential modeling mamba for 3d medical image segmentation,” in *Medical Image Computing and Computer Assisted Intervention – MICCAI 2024: 27th International Conference, Marrakesh, Morocco, October 6–10, 2024, Proceedings, Part VIII*, Berlin, Heidelberg, 2024, p. 578–588, Springer-Verlag.
  - [16] Abdelrahman Shaker, Syed Talal Wasim, Salman Khan, Jürgen Gall, and Fahad Shahbaz Khan, “Groupmamba: Efficient group-based visual state space model,” 2025.
  - [17] Maruf Adewole, Jeffrey D Rudie, Anu Gbdamosi, Oluyemisi Toyobo, Confidence Raymond, Dong Zhang, Olubukola Omidiji, Rachel Akinola, Mohammad Abba Suwaid, Adaobi Emegoakor, et al., “The brain tumor segmentation (brats) challenge 2023: glioma segmentation in sub-saharan africa patient population (brats-africa),” *ArXiv*, 2023.
  - [18] Abhijeet Parida, Daniel Capellán-Martín, Zhifan Jiang, Austin Tapp, Xinyang Liu, Syed Muhammad Anwar, María J Ledesma-Carbayo, and Marius George Linguraru, “Adult glioma segmentation in sub-saharan africa using transfer learning on stratified finetuning data,” *arXiv preprint arXiv:2412.04111*, 2024.
  - [19] Sarim Hashmi, Juan Lugo, Abdelrahman Elsayed, Dinesh Saggurthi, Mohammed Elseiagy, Alikhan Nurkamal, Jaskaran Walia, Fadillah Adamsyah Maani, and Mohammad Yaqub, “Optimizing brain tumor segmentation with mednext: Brats 2024 ssa and pediatrics,” *arXiv preprint arXiv:2411.15872*, 2024.
  - [20] Ahmed Jaheen, Abdelrahman Elsayed, Damir Kim, Daniil Tikhonov, Matheus Scatolin, Mohor Banerjee, Qiankun Ji, Mostafa Salem, Hu Wang, Sarim Hashmi, et al., “Emednext: An enhanced brain tumor segmentation framework for sub-saharan africa using mednext v2 with deep supervision,” *arXiv preprint arXiv:2507.23256*, 2025.
  - [21] Aaron Defazio, Xingyu Yang, Harsh Mehta, Konstantin Mishchenko, Ahmed Khaled, and Ashok Cutkosky, “The road less scheduled,” *Advances in Neural Information Processing Systems*, vol. 37, pp. 9974–10007, 2024.
  - [22] The MONAI Consortium, “Project monai,” Dec. 2020.
  - [23] Ali Hatamizadeh, Vishwesh Nath, Yucheng Tang, Dong Yang, Holger R Roth, and Daguang Xu, “Swin unetr: Swin transformers for semantic segmentation of brain tumors in mri images,” in *International MICCAI brainlesion workshop*. Springer, 2021, pp. 272–284.
  - [24] Andriy Myronenko, “3d mri brain tumor segmentation using autoencoder regularization,” in *International MICCAI brainlesion workshop*. Springer, 2018, pp. 311–320.